processes

MDPI

Article

Experimental Design Modelization and Optimization of Pickling Process Parameters for Corrosion Inhibition in Steel Construction

Moussa Ouakki [1], Khaoula Alaoui [2,*], Radouane Lachhab [2], Mohamed Rbaa [3], Mohamed Cherkaoui [1], Mohamed Ebn Touhami [2] and Younes El Kacimi [2,*]

[1] National Higher School of Chemistry (NHSC), University Ibn Tofail, Kenitra BP. 133-14000, Morocco; moussa.ouakki@uit.ac.ma (M.O.); mohamed.cherkaoui@uit.ac.ma (M.C.)
[2] Laboratory of Advanced Materials and Process Engineering, Faculty of Sciences, University Ibn Tofail, Kenitra P.O. Box 133-14000, Morocco; mohamed.ebntouhami@uit.ac.ma (M.E.T.)
[3] The Higher Institute of Nursing Professions and Health Techniques of Casablanca, Casablanca P.O. Box 622-20250, Morocco; mohamed.rbaa@uit.ac.ma
* Correspondence: khaoula.alaoui@uit.ac.ma (K.A.); elkacimiyounes@yahoo.fr (Y.E.K.)

Abstract: The present study attempted to investigate the best conditions to use *2-(4-chlorophenyle)-1,4,5-triphenyle-H-imidazole* as a corrosion inhibitor of mild steel in a 7% HCl and 20% H_2SO_4 pickling bath mixture, using chemical, electrochemical, and surface response methodologies in a spherical field. For this, a Doehlert matrix and two principal factors of the Pickling Process were examined. An experimental evaluation was carried out using weight loss, electrochemical impedance spectroscopy, and polarization curve measurements. Impedance diagrams and Bode plots for uninhibited and inhibited systems were analyzed and simulated using the Z-view program, the fitted data obtained closely followed the same pattern as the experimental results. This study demonstrates that the *2-(4-chlorophenyle)-1,4,5-triphenyle-H-imidazole* compound is an effective inhibitor for mild steel in pickling bath solutions, and corrosion inhibition efficiency increases with increases in inhibitor concentration to attain 93.2% imidazole at 10^{-3} M. This is due to the absorbability of Cl^- and SO_4^{2-} present in the pickling bath solution and the synergistic effect between both elements. The response used in the exploitation of the design was the determination of inhibitor efficiency. This was assessed through weight loss measurements and electrochemical studies on samples in the absence and presence of *2-(4-chlorophenyle)-1,4,5-triphenyle-H-imidazole*. It has been shown that the compound under investigation is an effective cathodic-type inhibitor of mild steel corrosion in pickling bath mixtures. Therefore, the inhibition efficiency was improved with the concentration of the inhibitor, which depended on the molecular structure. The optimal corrosion inhibition efficiency as a function of variation in *2-(4-chlorophenyle)-1,4,5-triphenyle-H-imidazole* concentration and pickling bath temperature was simulated and demonstrated using canonical analysis; the obtained efficiency at 324 K for 6 h was 81.3% for the coded variable and 83.4% for the real variable. The experimental results are based on a real-time system and provide much more precise results than the simulated results.

Keywords: experimental designs; corrosion inhibition; modelization; optimization; matrix of Doehlert; gravimetric; electrochemical measurements; imidazole

check for updates

Academic Editors: Qunjie Xu and Wei Liang

Received: 10 January 2025
Revised: 25 February 2025
Accepted: 7 March 2025
Published: 9 March 2025

Citation: Ouakki, M.; Alaoui, K.; Lachhab, R.; Rbaa, M.; Cherkaoui, M.; Ebn Touhami, M.; El Kacimi, Y. Experimental Design Modelization and Optimization of Pickling Process Parameters for Corrosion Inhibition in Steel Construction. *Processes* **2025**, *13*, 796. https://doi.org/10.3390/pr13030796

Copyright: © 2025 by the authors. Licensee MDPI, Basel, Switzerland. This article is an open access article distributed under the terms and conditions of the Creative Commons Attribution (CC BY) license (https://creativecommons.org/licenses/by/4.0/).

1. Introduction

To remove surface scales, metals are submerged in acid pickling baths, which typically contain an appropriate acid solution. The acid reacts with and dissolves these scales. However, once they are removed, it can also begin to degrade the underlying metal. Moreover, corrosion frequently causes large financial losses and possible security issues, which is why different researchers are interested in protection technology [1–3]. Consequently, to mitigate this issue, the development of effective corrosion inhibitors has become a key area of research. Chemical substances, typically organic compounds, are employed as corrosion inhibitors form a protective barrier on metal surfaces, reducing the interaction between the metal and the corrosive environment [4–6]. The synthetic inhibitors linked to high electron (in charge) density prolong conjugation and exhibit polar functional groups, such as –CN, –OH, and –NH, which provide strong metal inhibitor bondings [7–11]. Heteroatoms (P, O, S, and N) transfer their electrons and/or charge to metallic d-orbitals, forming an efficient metal protective layer by coordinate bonding (chemisorption mechanism) [12–14]. Furthermore, the presence of homo-atomic or hetero-atomic multiple bonds enhances the adsorption ability of the inhibitor molecules by increasing their electron-donating ability through extensive conjugation [15–18]. The compound selected, namely "2-(4-chlorophenyl)-1,4,5-triphenyl-1H-imidazole", has the following traits:

(i) Organic compounds with aromatic rings containing electronegative functional groups and π-electrons in conjugated double bonds.
(ii) Specific interactions between functional groups containing nitrogen heteroatoms with free lone pairs of electrons and the metal surface, which can play an important role in inhibition.

Acid pickling inhibitors are expected to be chemically stable in order to provide high protective efficiency [19,20]. A multitude of studies have been conducted on the impact of temperature on acidic corrosion and the inhibition of corrosion in iron and steel, mostly in acidic environments.

Inhibitors' performance dependence on temperature and the comparison of thermodynamic data acquired from the corrosion process, with and without inhibitors, led to some conclusions regarding the mechanism of the inhibition effect [21–24].

A comparison of the corrosion inhibition performance of some substituted *1,4,5-triphenyl-1H-imidazole* compounds of mild steel in 0.5 M sulfuric acid and 1.0 M chloride acid was investigated using DFT, electrochemical, and weight loss methods [25]. It has been revealed that this compound exhibits mixed-type inhibitory behavior and provides excellent resistance. As the concentration of inhibitors increases, inhibition efficiency increases too. The kinetic and thermodynamic parameters that regulate the adsorption process are calculated and examined. For both neutral and protonated forms, DFT computations are performed at the B3LYP stages of theory using the 6–31G (d,p) basis for the gas and aqueous phases [26]. The correlation between corrosion inhibition and global reactivity descriptors is adequately analyzed and presented in the referenced study's section on quantum chemical computations.

This paper aims to continue these studies by investigating the corrosion inhibition performance of *2-(4-chlorophenyle)-1,4,5-triphenyle-H-imidazole* for mild steel in a new acidic pickling bath formula (a mixture of 7% HCl and 20% H_2SO_4). This paper subsequently explores the optimal response surfaces through a mathematical model adapted to the experimental data. Given the growing industrial demand, and for many other reasons, such as industrial efficiency and productivity, this process involves two principal stages:

(i) Conducting experiments at different points in this region and collecting data;
(ii) Predicting the results at other points by analyzing the reliability predictions.

Subsequently, the researcher will be positioned to ascertain whether the results of their system can be improved, as well as to what extent the specific values of the parameters should be utilized. Essentially, the response surface methodology is a framework employed to determine optimal experimental locations within the feasible region to enhance prediction accuracy wherever possible.

Once the researcher has defined the problem, the response surface methodology provides both alternative experimental strategies and evaluation criteria for the experimental domain and the response. The main advantage is that the process of fitting the experiment to the studied problem is completed before the experiment is performed. Adhering to this viewpoint, the most relevant optimality criteria are determined based on variance. Additionally, statistical validation of the empirical model is included.

2. Materials and Methods

2.1. Practical Conditions

The used steel specimens have a rectangular form with dimensions of 2.0 cm × 1.0 cm × 0.20 cm and the following chemical composition (wt%):

C, 0.17; Mn, 0.37; Si, 0.20; S, 0.03; P, 0.01; and balanced Fe. The specimen surfaces were polished using emery paper, then rinsed with distilled water, degreased with ethanol, and dried with hot air. For the weight loss measurements, the immersion period was 24 h at 298 ± 1 K. After immersion, the specimens were cleaned, and their weight was remeasured with an accuracy of 10^{-4} g to determine the corrosion rate [27]. The aggressive medium (7% HCl and 20% H_2SO_4 mixture) was prepared by diluting 98% H_2SO_4 and 37% HCl of analytical grade with distilled water. The molecular formula of the analyzed inhibitor, *2-(4-chlorophenyle)-1,4,5-triphenyle-H-imidazole*, is shown in Figure 1.

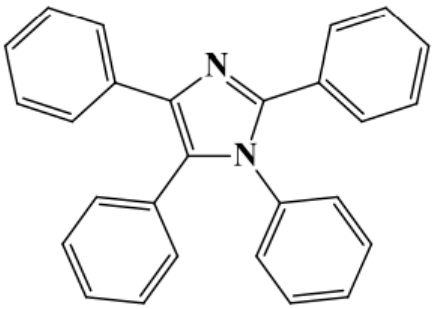


Figure 1. Corrosion inhibitor compound studied: *2-(4-chlorophenyle)-1,4,5-triphenyle-H-imidazole*.

The inhibition efficiency, E_{inh}(%), was calculated using following equation:

$$E_\omega\% = \frac{\omega^0_{corr} - \omega_{corr}}{\omega^0_{corr}} \times 100 \quad (1)$$

where $\omega^0{}_{corr}$ and ω_{corr} are the corrosion rates without and with inhibitors, respectively.

The electrolysis cell was protected by a cap with five apertures. The working electrode was pressure-fitted into a polytetrafluoroethylene holder exposing only 1 cm^2 of area to the aggressive solution. Potentiodynamic polarization studies were performed on mild steel specimens by automatically changing the electrode potential from −900 to −100 mV/Ag/AgCl versus OCP at a scan rate of 1 mVs^{-1}. The test solution was thermostatically controlled at 298 ± 1 K in an air atmosphere without bubbling. To evaluate the corrosion kinetic parameters, fitting with the Stern–Geary equation was used [18]. The

corrosion inhibition efficiency was evaluated from the corrosion current density values using the following relationship (2):

$$E_{PP}\% = \frac{i^0_{corr} - i_{corr}}{i^0_{corr}} \times 100 \quad (2)$$

where $i^0{}_{corr}$ and i_{corr} are, respectively, the corrosion current density values with and without inhibitors.

Finally, a transfer function analyzer employing a small amplitude a.c. signal (10 mV rms) was used to perform the electrochemical impedance spectroscopy measurements, covering a frequency range of 100 kHz to 100 mHz, with five points each decade. EC-Lab 10.3 (Orlando, FL, USA) software was then employed to evaluate the results in terms of an equivalent electrical circuit. The following equation below was used to determine the inhibition performance:

$$E_{EIS}\% = \frac{R^0_p - R_p}{R^0_p} \times 100 \quad (3)$$

where $R^0{}_p$ and R_p are the polarization resistance values without and with inhibitors, respectively.

To ensure reproducibility, all experiments were repeated three times, and the evaluated inaccuracy did not exceed 10%.

2.2. Design of Experiment Approach

Regarding the implementation of the experimental design, a matrix of Doehlert with two factors [19] was selected. The experimental points in the space of the coded variables were evenly distributed according to the Doehlert experiment matrices.

These experiment matrices allow for the step-by-step investigation of a second-degree response surface; this means that the field of study can be adjusted by recovering some of the experimental points employed in a previous study, or by adding new factors with new experimental points to the investigated design.

To measure how the variables affect the response, a second-degree polynomial model is created [19]:

$$Y = b_0 + b_1{*}X_1 + b_2{*}X_2 + b_{1\text{-}1}{*}(X_1{*}X_1) + b_{2\text{-}2}{*}(X_2{*}X_2) + b_{1\text{-}2}{*}(X_1{*}X_2) \quad (4)$$

where X_1 and X_2 are independent variables representing the inhibitor concentration and temperature of the pickling bath solution; b_0 is constant; b_1 and b_2 are coefficients reflecting the effect of factors X_1 and X_2; $b_{1\text{-}2}$ are coefficients reflecting the interaction between two factors X_1X_2; and $b_{1\text{-}1}$ and $b_{2\text{-}2}$ are coefficients reflecting the influence of quadratic X_1 and X_2.

2.3. Study Vicinity

Corrosion and corrosion inhibition were determined to be contingent upon concentration and temperature. Temperature and concentration significantly influence the rate of metal corrosion, and their variations serve as useful tools for investigating and elucidating the adsorption mechanism of an inhibitor. The variations in both influential elements for corrosion inhibition, such as (1) temperature and (2) inhibitor concentration, were selected to simulate the natural conditions encountered in the experimental field. The concentrations of the inhibitor, namely *2-(4-chlorophenyle)-1,4,5-triphenyle-H-imidazole*, were studied in the range 1 to 1000 µM, and a blank mixture solution was prepared for comparison. The influence of pickling bath temperature on the potentiodynamic polarization curves in the

absence and presence of the *2-(4-chlorophenyle)-1,4,5-triphenyle-H-imidazole* inhibitor was studied for mild steel in mixture solution in the range of 298 ± 2 K to 328 ± 2 K.

Classically, the various levels were expressed in a system of coded variables. Level +1 corresponded to the highest natural value and level −1 to the lowest natural value.

The correspondence between real variables and coded ones was ascertained starting from the following Equation (5):

$$X_j = \frac{U_j - U_j^0}{\Delta U_j} \quad (5)$$

where X_j is value of the variable factor in the *j*-coded variable; U_j is corresponding value of factor *j* in the natural variable; $U^0{}_j$ is the central value in the field of variation; and ΔU_j is variation pace.

$$\Delta U_j = \frac{U_j^{max} - U_j^{min}}{2} \quad (6)$$

All fields of variation for the 3 studied factors are detailed in Table 1.

Table 1. Center, variation step, and range of parameters studied.

	Factor	Unit	Range	Centre	Variation Step
U_1	Inhibitor concentration	µM	1 to 1000	500	500
U_2	Pickling bath temperature	K	298 ± 2 to 328 ± 2	318	10

2.4. Experimental Response

The current study's only experimental response was the inhibition efficiency of the mixture (E%); this can be calculated using the following Equation (7):

$$E\ \% = \frac{\nu_0 - \nu}{\nu_0} \quad (7)$$

where ν_0 and ν represent the weight loss of steel in the absence and presence of the inhibitor/mixture, respectively.

2.5. Design of Experiment Matrix

All tests were carried out in the presence or absence of an inhibitor. A point was also created in the center of the domain, which was repeated three times. Table 2 illustrates the Doehlert matrix design [20].

Table 2. Experimental matrix design and response vectors.

N° Exp	X_1	X_2	$X_{1\text{-}1}$	$X_{2\text{-}2}$	$X_{1\text{-}2}$
1	1.00000	0.00000	1.00000	0.00000	0.00000
2	−1.00000	0.00000	1.00000	0.00000	0.00000
3	0.50000	0.86603	0.25000	0.74996	0.43300
4	−0.50000	−0.86603	0.25000	0.74996	0.43300
5	0.50000	−0.86603	0.25000	0.74996	−0.43300
6	−0.50000	0.86603	0.25000	0.74996	−0.43300
7	0.00000	0.00000	0.00000	0.00000	0.00000

The use of coding factor relations permitted the transformation of the experience matrix into predicted experimentation designs. Table 2 presents the results of the inhibitor efficiency measurements for the different mixtures. To ensure reproducibility, all experiments were repeated three times and the evaluated inaccuracy did not exceed 3%.

3. Findings

3.1. Weight Loss Investigation

We began this investigation with a comparative weight loss study examining 0.5 M H_2SO_4 and a novel pickling bath solution, formulated with 7% HCl mixed with 20% H_2SO_4. The weight loss of mild steel corrosion in environments studied with and without different concentrations of the *2-(4-chlorophenyle)-1,4,5-triphenyle-H-imidazole* compound was determined after 6 h of immersion at 298 ± 2 K. The inhibition efficiencies represent a similar pattern (Figure 2); thus, at 10^{-3} M of *2-(4-chlorophenyle)-1,4,5-triphenyle-H-imidazole* compound, the maximum inhibition efficiency (E_ω = 96.7%) was obtained for the 0.5 M H_2SO_4 solution [7]. For the new pickling bath mixture, a slight variation in inhibition efficiency (E_ω = 93.2%) was observed, without any impact on its inhibition performance.

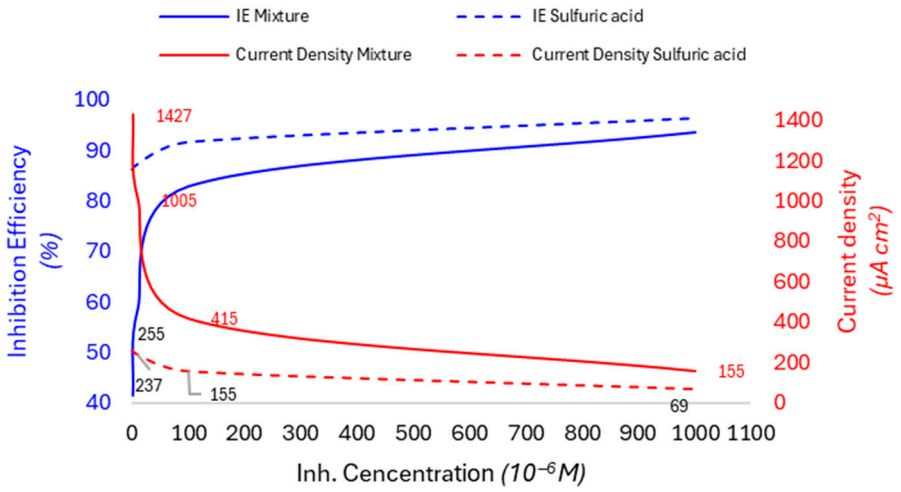


Figure 2. Comparison of corrosion rate, corrosion inhibition efficiency, and their evolution vs. concentration of *2-(4-chlorophenyle)-1,4,5-triphenyle-H-imidazole* determined after 6 h of immersion at 298 ± 2 K [7].

This result is best explained in terms of the absorbability of Cl^- and SO_4^{2-} and the synergistic effect between both elements [7,27–29]. In fact, anions with less hydration, for example chloride ions, are expected to have a higher specific adsorption. Being selectively adsorbed, they provide an excess of negative charge in the solution phase, favoring the additional adsorption of imidazole compounds and resulting in higher inhibition [7,30–33]. It is demonstrated during this study that these compounds are good inhibitors for mild steel corrosion in both the environment of 0.5 M H_2SO_4 and in the novel pickling bath solution formulated with 7% HCl mixed with 20% H_2SO_4.

3.2. Electrochemical Investigation—Current Potential

Polarization curves of the mild steel electrode in the novel pickling bath solution formulated on the basis of 7% HCl mixed with 20% H_2SO_4, without and with the addition of *2-(4-chlorophenyle)-1,4,5-triphenyle-H-imidazole* at different concentrations, are presented in Figure 3, and their obtained corrosion parameters are provided in Table 3. As it can be seen, both cathodic and anodic reactions of mild-steel electrode corrosion were inhibited by the increase in imidazole compound concentration (7% HCl + 20% H_2SO_4 mixture). It is clear that the studied imidazole compound suppressed the cathodic reaction to greater extents than the anodic one, especially at low concentration.

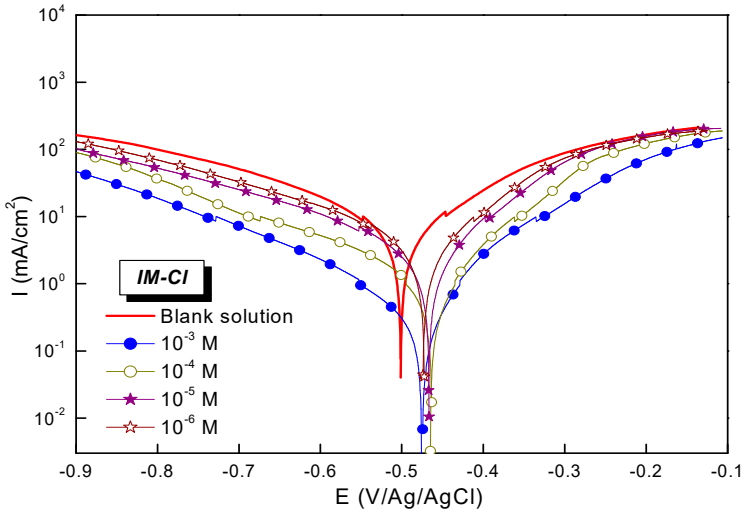


Figure 3. Polarization curves for mild steel in 7% HCl + 20% H_2SO_4 mixture without and with diverse concentrations of *2-(4-chlorophenyle)-1,4,5-triphenyle-H-imidazole* at 298 ± 2 K.

Table 3. Corrosion parameters obtained from potentiodynamic polarization measurements of mild steel in 7% HCl + 20% H_2SO_4 mixture without and with different concentrations of *2-(4-chlorophenyle)-1,4,5-triphenyle-H-imidazole*.

Solution	*Conc* (10^{-6} M)	E_{corr} (mV/Ag-AgCl)	i_{corr} (μA cm^2)	$-\beta_c$ (mV dec^{-1})	β_a (mV dec^{-1})	E_{pp} (%)
Blank	0	499	2436	125	136	--
Inhibited	1	470	1427	131	136	41.4
Inhibited	10	463	1005	129	121	58.7
Inhibited	100	461	415	126	108	82.9
Inhibited	1000	474	155	127	120	93.6

This result suggests that the addition of *2-(4-chlorophenyle)-1,4,5-triphenyle-H-imidazole* reduces anodic dissolution and retards the hydrogen evolution reaction. Tafel lines of nearly equal slopes were obtained, indicating that the hydrogen evolution reaction was activation-controlled.

The corrosion current density (I_{corr}) values for both solutions (0.5 M H_2SO_4 and 7% HCl + 20% H_2SO_4 mixture) are presented in Figure 4; the data show that I_{corr} values decreased significantly in the presence of *2-(4-chlorophenyle)-1,4,5-triphenyle-H-imidazole* and further decreased with increasing inhibitor concentration in both solutions. No definite trend was observed in the shift in E_{corr} values in the presence of various concentrations of the inhibitor in the 7% HCl + 20% H_2SO_4 mixture.

In the anodic domain, we observed that the presence of *2-(4-chlorophenyle)-1,4,5-triphenyle-H-imidazole* in the acidic mixture reduced the anodic current density. This result indicates that these inhibitors exhibit both cathodic and anodic inhibition effects.

Therefore, *2-(4-chlorophenyle)-1,4,5-triphenyle-H-imidazole* can be classified as an inhibitor of relatively mixed effect (anodic/cathodic inhibition) in the 7% HCl + 20% H_2SO_4 mixture. It is also apparent that the inhibition efficiency (η_{PP}) followed the same order as that found by the weight loss measurements.

According to the results presented in Table 3, it can be seen that for the studied imidazole inhibitor, η(%) increases with the increase in inhibitor concentration, reaching a maximum value of 10^{-3} M.

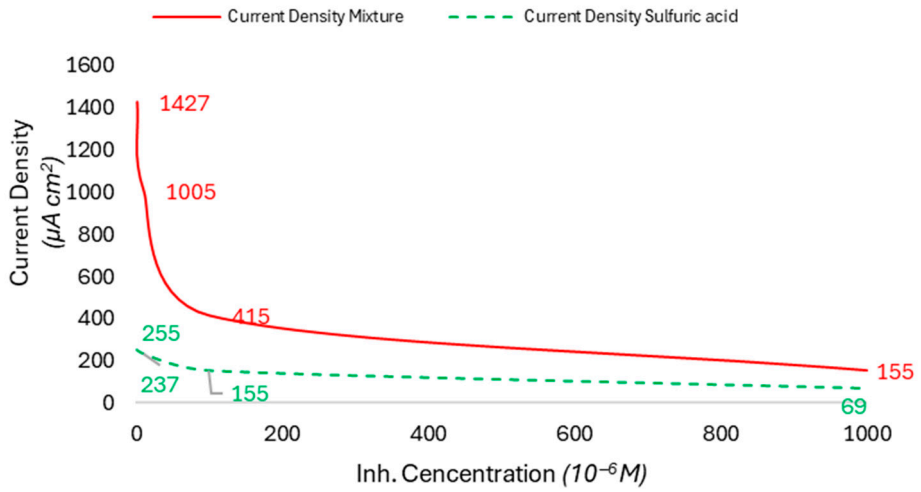


Figure 4. Comparison of corrosion current density (I_{corr}) of mild steel in 0.5 M sulfuric acid and 7% HCl + 20% H_2SO_4 mixture containing different concentrations of *2-(4-chlorophenyle)-1,4,5-triphenyle-H-imidazole* at 298 ± 2 K.

This shows that the addition of these compounds does not modify the hydrogen evolution mechanism. The reduction in H^+ ions at the mild steel surface takes place mainly through a charge transfer mechanism [25,30]. On the other hand, the branches correlated to the anodic reaction changed noticeably, indicating that the iron dissolution mechanism varied after the dissolution of the tested imidazole compound [32–34]. The interpretation of these cures shows that both reactions (i.e., anodic and cathodic) affect the corrosion process, but the cathodic reaction is more pronounced than the anodic reaction.

The shifts or displacements in E_{corr} values when the results in the blank acid mixture solution are compared with the inhibited ones are generally less than 85 mV. This suggests that these studied compounds inhibit both the anodic and cathodic reactions involved in the corrosion of mild steel in acid mixture solutions, and they are therefore mixed-type inhibitors [35–37]. Also, we can deduct from current-potential data that the adsorption at higher concentrations of the explored inhibitor is probably extremely effective, covering the steel surface almost entirely, resulting in important inhibitory effects [38,39]. Higher concentrations can result in a multilayer adsorption, leaving no part of the mild steel surface unprotected and blocking all active sites.

3.3. Electrochemical Impedance Spectroscopy

Figure 5 below illustrates the Nyquist plots obtained for mild steel in the blank and inhibitor solutions (7% HCl + 20% H_2SO_4 mixture). The observed spectrum consists of capacitive loops associated with the transferred charges, with the diameter increasing significantly after the addition of the inhibitor, reaching a maximum at 10^{-3} M of *2-(4-chlorophenyle)-1,4,5-triphenyle-H-imidazole*.

A depressed semicircle of charge transfer was observed, with the peak of the semicircle plot shifted towards high frequencies; this is associated with a single time constant in the Bode plot [40–44]. The low-frequency inductive loop can be attributed to the relaxation process acquired by adsorption species such as $SO_4^{2-}{}_{ads}$ and $H^+{}_{ads}$ on the electrode surface [45]. The diameter of the semicircular Nyquist plot rises with increasing inhibitor concentration.

Impedance spectroscopy parameters for mild steel in acidic mixtures with and without inhibitor addition are listed in Table 4. The electrochemical data obtained from the Nyquist plot were fitted, and the proposed equivalent circuit is shown below. It is made up of solution resistance identified by R_s, the charge-transfer resistance given by R_{ct}, and a

constant phase element. Impedance results were analyzed using the Z-view program, and the obtained Bode plots exhibit three distinctive segments for the mild steel/imidazole/acid mixture (Figures 6 and 7).

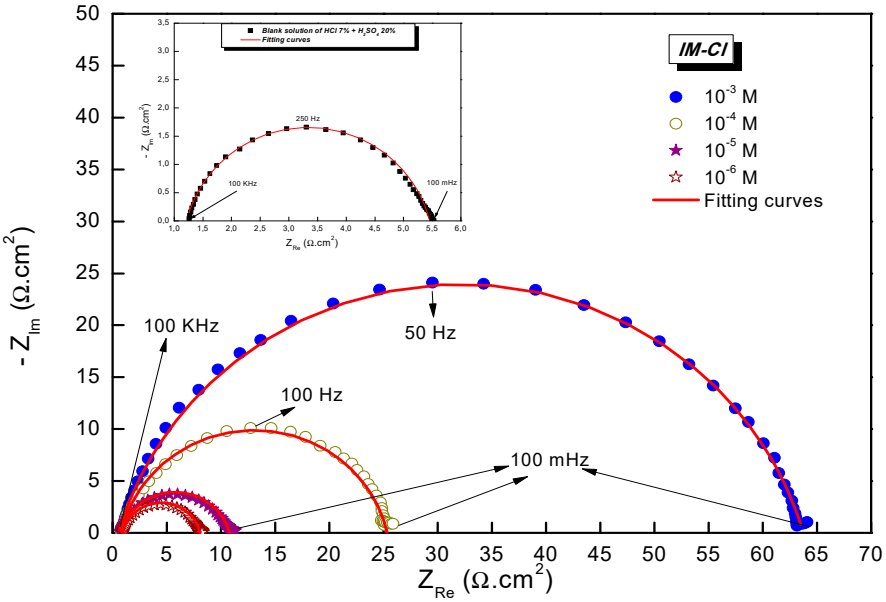


Figure 5. Nyquist diagrams obtained for blank and inhibited solutions (7% HCl + 20% H_2SO_4 mixture/*2-(4-chlorophenyle)-1,4,5-triphenyle-H-imidazole*) for mild steel at 298 ± 2 K.

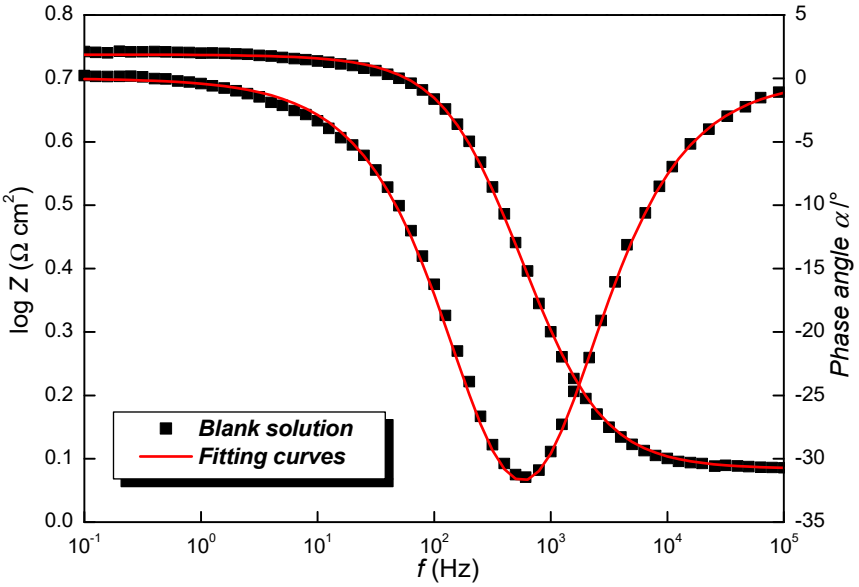


Figure 6. Bode plot of mild steel in blank solution: 7% HCl + 20% H_2SO_4 mixture at T = 298 ± 2 K. Comparison of experimental (scatter) and fitting (red line) data.

From Table 4, it can be observed that R_{ct} increased with increases in inhibitor concentration. This can be attributed to the formation of an isolating protective film at the metal/solution interface. In addition, it can be observed that an increase in the concentration of the imidazole inhibitor causes a decrease in the double layer capacity (C_{dl}), which confirms that the studied inhibitor adsorbs on the mild steel surface; this situation is due to an increase in surface coverage by the inhibitor molecules, which leads to an increase in inhibition efficiency [46–48]. We can also observe that the inhibition efficiency (η_{EIS}%) improves with increasing imidazole concentration up to 93.3% at 10^{-3} M.

Table 4. Impedance spectroscopy parameters for mild steel in 7% HCl + 20% H_2SO_4 mixture in blank solution and with addition of various concentrations of *2-(4-chlorophenyle)-1,4,5-triphenyle-H-imidazole* at 298 ± 2 K.

Solution	*Conc* (10^{-6} M)	R_s (Ω cm^2)	R_{ct} (Ω cm^2)	C_{dc} (μF cm^{-2})	n_{dl}	Q (μF Sn^{-1})	η_{EIS} (%)
Blank	0	1.2 ± 0.3	4.2 ± 0.1	157.0	0.844 ± 0.03	489.8 ± 0.5	-
Inhibited	1	0.9 ± 0.3	7.2 ± 0.2	94.3	0.863 ± 0.02	255.9 ± 0.4	40.8
Inhibited	10	0.7 ± 0.3	10.0 ± 0.3	93.1	0.845 ± 0.03	250.3 ± 0.3	57.7
Inhibited	100	0.7 ± 0.3	24.5 ± 0.4	53.8	0.863 ± 0.01	133.0 ± 0.4	82.7
Inhibited	1000	0.5 ± 0.2	63.2 ± 0.5	45.0	0.826 ± 0.02	127.4 ± 0.3	93.3

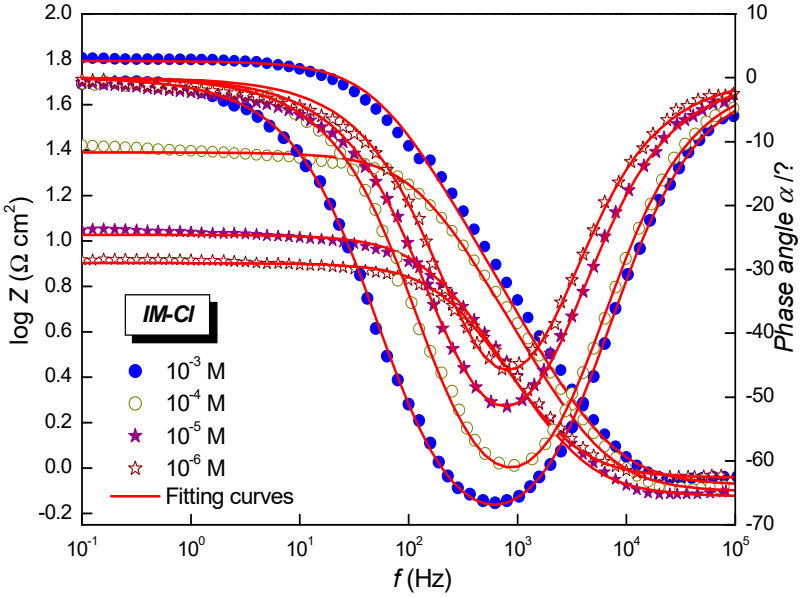


Figure 7. Bode plot of mild steel in 7% HCl + 20% H_2SO_4 mixture in the presence of various concentrations of *2-(4-chlorophenyle)-1,4,5-triphenyle-H-imidazole* at T = 298 ± 2 K. Comparison of experimental (scatter) and fitting (red line) data.

On the other hand, the inhibition efficiency of the organic compounds mostly depends on their size and active centers. The best performance of the compound *2-(4-chlorophenyle)-1,4,5-triphenyle-H-imidazole* may be attributed to the presence of nitrogen atoms based on heterocyclic compounds and the benzene rings attached to the imidazole ring via a methylene group.

Figure 8 shows the electrical equivalent circuit employed to analyze the impedance plots.

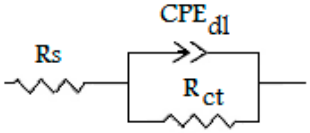


Figure 8. Proposed electrical equivalent circuits.

3.4. Statistical Treatment

In this investigation, the statistical analysis consisted of assessing the gap between the experimental and mathematical models using chemometric tools such as Nemrodw software. Tests of multiple regressions allowed the mathematical equation below.

$$Y = 81.0 + 24.0X_1 - 0.1X_2 - 14.0X_1X_1 - 3.3X_2X_2 + 4.6X_1X_2 \quad (8)$$

3.5. Validity of the Model

The statistical analyses that led to establishing the validity of the model are displayed in the form of variance analysis in Table 5.

Table 5. Analysis of variance (ANOVA) for the response model.

Source of Variation	*Sum of Squares*	*Degree of Freedom*	*Mean Square*	*Ratio*	*Significance of Regression Coefficients*
Regression	1.8937×10^3	5	2.7874×10^2	51.20	<0.001
Residues	20.4	1	20.4	-	-
Validity	112.3	1	31.21	12.25	<0.01
Error	2.13	2	1.24	-	-
Total	1.9177×10^3	9	-	-	-

This table provides the percentage of variance explained by the mathematical model in comparison to the variance contained within the experimental results. A probability of ANOVA smaller than 5% confirmed the validity of the suggested model.

3.6. Residual Analysis

Residuals are the deviations of the observed values of the dependent variable from the predicted values for the current model. The residual analysis is displayed in Table 6 below.

Table 6. Residual deviations of the observed and predicted values identified using design of experiment.

N° Experience	$Y_{exp.}$ *(%)*	$Y_{cal.}$ *(%)*	*Deviation*	*Standard Deviation*	*dU*
1	93.1	91.2	1.9	−0.103	0.180
2	41.3	43.7	−2.4	−0.120	0.236
3	87.2	89.1	−1.9	−0.283	0.152
4	67.6	65.6	2.0	0.244	0.352
5	83.4	85.4	−2.0	−0.771	0.311
6	63.1	61.3	1.8	−0.010	0.710
7	81.7	81.5	0.2	0.182	0.560

The ANOVA models used to analyze the responses of the dependent variable in most of the programs in the Experimental Design module make certain assumptions about the distribution of the residual (but not predicted) values of the dependent variable. These assumptions can be summarized by saying that the ANOVA model assumes normality, linearity, heteroscedasticity, and the independence of residuals. These kinds of properties-dof residuals for a dependent variable can be inspected using the options and selections available in the Experimental Design module.

The predicted vs. residual values plot shows that the relation between the residual and predicted values is clearly uniform. Fortunately, the uniformity of the residual vs. deleted residual results provide a serial correlation between these marginal means and standard deviations, confirming that the modelization and experimental data are nearly perfect.

3.7. Graphic Analysis of the Model

The aim of this study was to find an inhibitor solution whose features could have been previously defined from the operative conditions extracted from the mathematical model.

Because the direct exploitation of the equation was delicate, it was convenient to restore it under a graphic representation. While fixing two of the four factors of the survey, it was possible to represent the response surface, which resulted in a surface of regression

in a three-dimensional space. It was also possible to project the equation of the design under the isoresponse curves, interpreted at the card curves level.

3.8. Evolution of Efficiency as a Function of Inhibitor Concentration and Temperature

Figure 9 represents the evolution of efficiency as a function of temperature and inhibitor efficiency. This figure shows that the inhibitor efficiency increased when the temperature increased. This evolution was, however, more accentuated for the weakest concentrations of inhibitors. The simulation plot and response surface plot are shown in Figure 10, and the maximum inhibition efficiency as a function of the variation in both factors was studied.

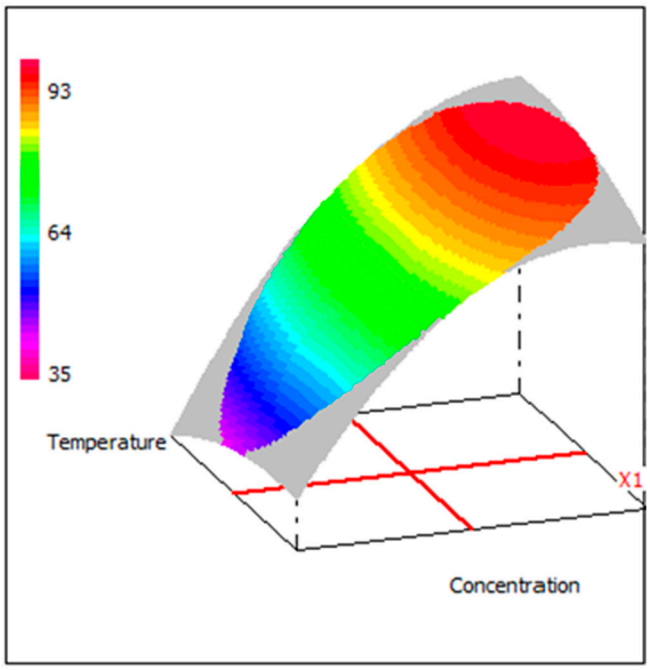


Figure 9. Surface response plot proving the variation in inhibition efficiency as a function of *2-(4-chlorophenyle)-1,4,5-triphenyle-H-imidazole* concentration (X_1) and temperature (X_3). The submersion time (X_2) is fixed at 6 h.

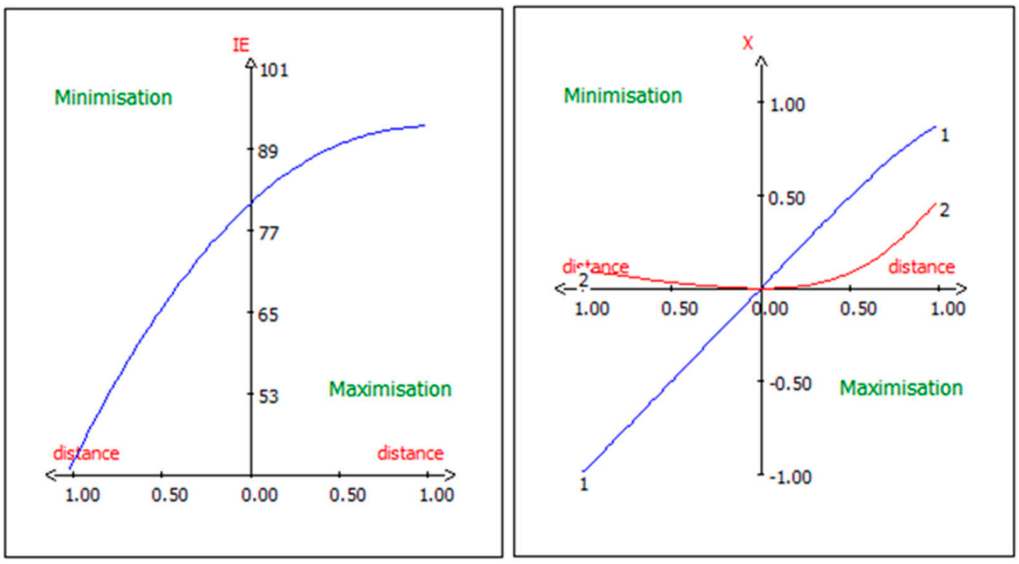


Figure 10. Simulation and response surface plot showing the maximum inhibition efficiency as a function of variation in the factors studied.

3.9. Canonical Correlation Analysis

Canonical correlation analysis was used to determine and measure the relationships between the two sets of variables studied: corrosion inhibitor concentration and acidic pickling bath temperature. It is especially pertinent in the same situations as multiple regression, when there are multiple intercorrelated outcome variables. Canonical correlation analysis allows us to determine a set of canonical variates, that is, orthogonal linear combinations of the variables within each group, that best explain the variability both within and between groups.

Canonical analysis is a method of rewriting a second-degree equation in a form in which it can be more readily understood. Assume that the estimated response is fitted by a second-order model as follows:

$$\hat{y} = b_0 + \sum_{j=1}^{k} b_j x_j + \sum_{i \geq j} \sum b_{ij} x_i x_j \tag{9}$$

Given the matrices

$$x = \begin{pmatrix} x_1 \\ \vdots \\ x_k \end{pmatrix}, \; b = \begin{pmatrix} b_1 \\ \vdots \\ b_k \end{pmatrix}, \quad B = \begin{pmatrix} b_{11} & \frac{1}{2}b_{12} & \cdots & \frac{1}{2}b_{1k} \\ \frac{1}{2}b_{12} & b_{22} & & \frac{1}{2}b_{2k} \\ \vdots & & \ddots & \vdots \\ \frac{1}{2}b_{1k} & \frac{1}{2}b_{2k} & \cdots & b_{kk} \end{pmatrix} \tag{10}$$

Equation (9) is written as

$$\hat{y} = b_0 + x'b + x'Bx \tag{11}$$

Mathematically, a second-degree polynomial (Equation (11)) has a necessarily unique stationary point, S, that can be a maximum, a minimum, or a saddle point. By translation of the origin to the stationary point and rotation of the axes, Equation (11) becomes

$$\hat{y} = \hat{y}_s + \lambda_1 z_1^2 + \lambda_2 z_2^2 + \ldots + \lambda_k z_k^2 \tag{12}$$

which is known as the canonical equation. In Equation (12), $\hat{y}_s$ stands for the estimated value at the stationary point S, and λ_i, $i = 1,\ldots, k$, are the eigenvalues of the symmetric matrix B. The canonical coordinates, z, of point x are obtained as $z = M'(x - x_S)$, where M (by column) is the matrix of normalized eigenvectors of B, and x_S represents the coordinates of S.

Written as in Equation (13), the analysis of the quadratic equation is very simple. If all the coefficients (λ_i, $i = 1,\ldots, k$) are positive, the stationary point S is a minimum; if all the coefficients are negative, S is a maximum; and if some coefficients are positive and other negatives, S is a saddle point. We illustrate this analysis with Example 1. The second-order fitted model is as follows:

$$\hat{y} = 82.34 + 5.27x_1 + 21.53x_2 - 2.87x_1^2 - 13.54x_2^2 - 3.465x_1x_2 \tag{13}$$

The contour lines of this surface are shown in Figure 11, and the canonical equation is

$$\hat{y} = 81.00 + 4.75\, z_1 + 23.44\, z_2 - 3.16\, z_1^2 - 15.01\, z_2^2 \tag{14}$$

Thus, the graphical representation of the optimum corrosion inhibition of *2-(4-chlorophenyle)-1,4,5-triphenyle-H-imidazole*, determined on the basis of canonical analysis, is displayed below (Figure 11).

Therefore, the stationary point S is the maximum, as we also observe in Figure 12.

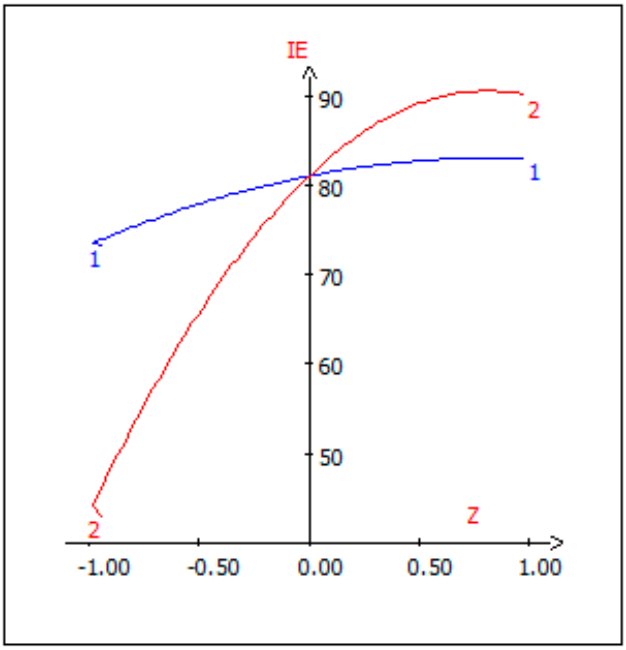


Figure 11. Simulation plot using canonical analysis showing the optimum corrosion inhibition efficiency as a function of variation in the two factors studied (*2-(4-chlorophenyle)-1,4,5-triphenyle-H-imidazole* concentration and pickling bath temperature).

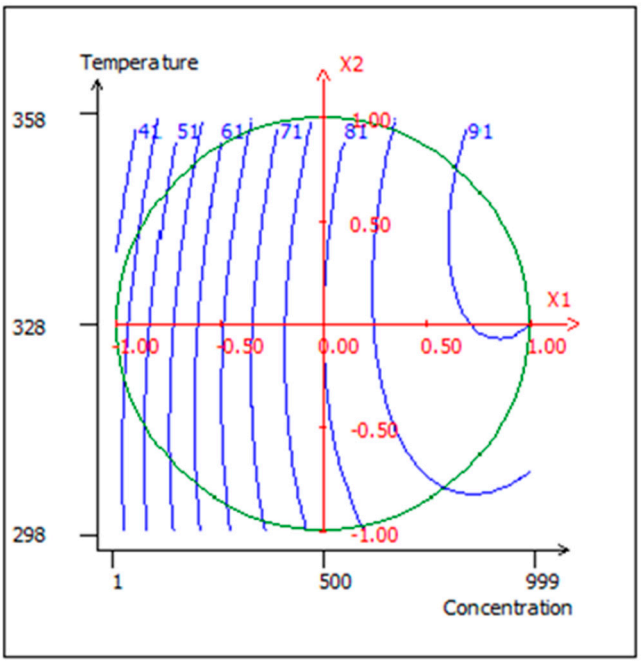


Figure 12. Level curves of the second-order model fitted with data from Example 1 (S: stationary point).

The $z = M'(x - x_S)$ transformation is

$$Z_1 = 0.207\ x_1 - 0.978\ x_2 \quad (15)$$

$$Z_2 = 0.978\ x_1 - 0.207\ x_2 \quad (16)$$

and its inverse is

$$x_1 = 0.21\ z_1 + 0.98\ z_2 \quad (17)$$

$$x_2 = -0.98\, z_1 - 0.21\, z_2 \quad (18)$$

If $z_1 = z_2 = 0$ in the system of Equations (17) and (18), the coordinates of the stationary point x_S are obtained. Again, this information is also seen in Figure 11. The estimated response in S, $\hat{y}_s$, is 81% (independent term in Equation (14)).

The eigenvectors associated with the eigenvalues are $(0.207, -0.978)'$ and $(-0.978, -0.207)'$, which are the coefficients of x_1 and x_2, respectively, in Equations (15) and (16).

The boxplots displayed below in Figure 13 also confirm the canonical correlation obtained.

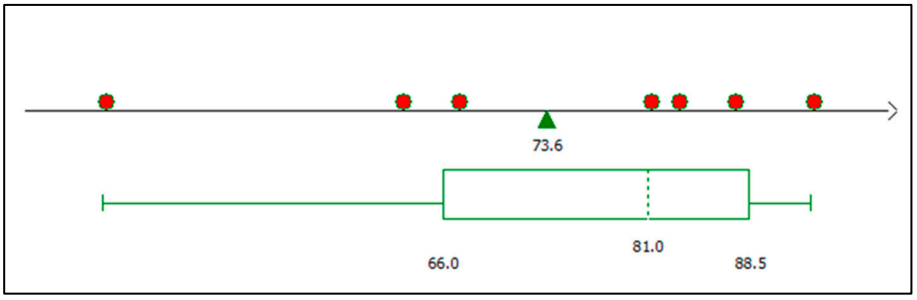


Figure 13. Boxplots obtained from experimental design showing the optimum corrosion inhibition efficiency as a function of variation in the two factors studied (*2-(4-chlorophenyle)-1,4,5-triphenyle-H-imidazole* concentration and pickling bath temperature).

4. Conclusions

The inhibiting properties of this film generally remain independent of variations in the concentration of hydrochloric acid pickling baths. It is demonstrated during this study that the *2-(4-chlorophenyle)-1,4,5-triphenyle-H-imidazole* compound is a good inhibitor for mild steel in pickling bath solutions, and corrosion inhibition efficiency increases with the increase in inhibitor concentration to attain 93.2% imidazole at 10^{-3} M. This is due to the absorbability of Cl^- and SO_4^{2-}, present in the pickling bath solution, and the synergistic effect between these elements.

In fact, anions with less hydration of chloride ions are expected to have a higher specific adsorption. Being selectively adsorbed, they provide an excess of negative charge in the pickling bath solution phase, favoring the additional adsorption of *2-(4-chlorophenyle)-1,4,5-triphenyle-H-imidazole* compounds and resulting in higher inhibition.

The surface response methodology was used to find out the best conditions for *2-(4-chlorophenyle)-1,4,5-triphenyle-H-imidazole* as a corrosion inhibitor of mild steel, considering low and high levels of pickling hydrochloric acidic solution. Impedance diagrams and Bode plots for uninhibited and inhibited systems were analyzed and simulated using the Z-view program. The fitted data obtained trends with nearly the same patterns as the experimental results.

The experiment design methodology has enabled us, through a limited number of carefully selected tests, to obtain a description of the studied response behavior within the experimental area, and thus determine the experimental conditions that maximize the efficiency of inhibition. In this regard, the obtained efficiency at 324 K for 6 h for the coded variable was 81.3%, and 83.4% for the real variable.

Author Contributions: M.O.: Data curation, Formal analysis, Methodology, Visualization, Writing—original draft. K.A.: Conceptualization, Data curation, Formal analysis, Investigation, Methodology, Supervision, Validation, Visualization, Writing—review and editing. R.L. and M.R.: Data curation, Formal analysis. M.C. and M.E.T.: Funding acquisition, Investigation, Project administration, Resources, Software, Supervision, Validation. Y.E.K.: Data curation, Methodology, Project administra-

tion, Resources, Software, Writing—original draft, Writing—review and editing. All authors have read and agreed to the published version of the manuscript.

Funding: This research received no external funding.

Data Availability Statement: The authors appreciate the experimental support given by Ibn Tofail University, who provided materials for all tests.

Acknowledgments: The authors appreciate the experimental support given by Ibn Tofail University, who provided materials for all tests.

Conflicts of Interest: The authors have declared that there are no conflicts of interest.

References

1. Alaoui, K.; Kaya, S.; Salim, R.; Kamal, A.; Moussaoui, A.; Habsaoui, A.; Touhami, M.E.; El Kacimi, Y. Correlation between halogens atoms elements, their positions on the main chain of organic compounds, and corrosion inhibition performance. In *Handbook of Research on Corrosion Sciences and Engineering*; IGI Global: Hershey, PA, USA, 2023; pp. 65–84. [CrossRef]
2. Hussin, M.H.; Kassim, M.J.; Razali, N.; Dahon, N.; Nasshorudin, D. The effect of Tinospora crispa extracts as a natural mild steel corrosion inhibitor in 1M HCl solution. *Arab. J. Chem.* **2016**, *9*, S616–S624. [CrossRef]
3. Abboud, Y.; Abourriche, A.; Saffaj, T.; Berrada, M.; Charrouf, M.; Bennamara, A.; Al Himidi, N.; Hannache, H. 2,3-Quinoxalinedione as a novel corrosion inhibitor for mild steel in 1M HCl. *Mater. Chem. Phys.* **2007**, *105*, 1–5. [CrossRef]
4. James, A.O.; Oforka, N.C.; Abiola, O.K. Inhibition of acid corrosion of mild steel by pyridoxal and pyridoxol hydrochlorides. *Int. J. Electrochem. Sci.* **2007**, *2*, 278–284. [CrossRef]
5. Ebenso, E.E. Inhibition of corrosion of mild steel hydrochloric acid by some azo dyes. *Niger. J. Chem. Res.* **2001**, *6*, 8–12. [CrossRef]
6. Elkacimi, Y.; Achnin, M.; Aouine, Y.; E Touhami, M.; Alami, A.; Touir, R.; Sfaira, M.; Chebabe, D.; Elachqar, A.; Hammouti, B. Inhibition of Mild Steel Corrosion by some Phenyltetrazole Substituted Compounds in Hydrochloric Acid. *Port. Electrochim. Acta* **2012**, *30*, 53–65. [CrossRef]
7. Ouakki, M.; Galai, M.; Rbaa, M.; Abousalem, A.S.; Lakhrissi, B.; Rifi, E.H.; Cherkaoui, M. Investigation of imidazole derivatives as corrosion inhibitors for mild steel in sulfuric acidic environment: Experimental and theoretical studies. *Ionics* **2020**, *26*, 5251–5272. [CrossRef]
8. Liu, Y.; Liu, J.; Chen, B.; Ren, X. Investigation of three betaine surfactants and KI compounds as a corrosion inhibitor on carbon steel in industrial pickling. *J. Mol. Struct.* **2025**, *1328*, 141269. [CrossRef]
9. Li, W.; He, Q.; Pei, C.; Hou, B. Experimental and theoretical investigation of the adsorption behaviour of new triazole derivatives as inhibitors for mild steel corrosion in acid media. *Electrochim. Acta* **2007**, *52*, 6386–6394. [CrossRef]
10. Chaouche, R.; Tiskar, M.; Larhlid, I.; Ihamdane, R.; El Amri, A.; Mansour, A.A.; Hsissou, R.; Salghi, R.; Cheikhi, N.; Chaouch, A.; et al. Exploring of the Origanum Compactum essential oil as an ecofriendly corrosion inhibitor for mild steel in 1M HCl environment: Experimental, DFT, MD, DFTB and PDOS approaches. *J. Mol. Struct.* **2025**, *1327*, 141112. [CrossRef]
11. Zerga, B.; Attayibat, A.; Sfaira, M.; Taleb, M.; Hammouti, B.; Touhami, M.E.; Radi, S.; Rais, Z. Effect of some tripodal bipyrazolic compounds on C38 steel corrosion in hydrochloric acid solution. *J. Appl. Electrochem.* **2010**, *40*, 1575–1582. [CrossRef]
12. Scendo, M.; Hepel, M. Inhibiting properties of benzimidazole films for Cu(II)/Cu(I) reduction in chloride media studied by RDE and EQCN techniques. *Corros. Sci.* **2007**, *49*, 3381–3407. [CrossRef]
13. Larabi, L.; Benali, O.; Mekelleche, S.; Harek, Y. 2-Mercapto-1-methylimidazole as corrosion inhibitor for copper in hydrochloric acid. *Appl. Surf. Sci.* **2006**, *253*, 1371–1378. [CrossRef]
14. Belhadi, M.; Roby, O.; Chafi, M.; Lgaz, H.; Lee, H.-S.; Alzahrani, A.Y.; Tighadouini, S. Mechanistic Insights and Performance of Pyrazole-Based Corrosion Inhibitors for Carbon Steel in Acidic Media: Experimental and Computational Approaches. *J. Bio-Tribo-Corros.* **2025**, *11*, 16. [CrossRef]
15. Chugh, B.; Singh, A.K.; Chaouiki, A.; Salghi, R.; Thakur, S.; Pani, B. A comprehensive study about anti-corrosion behaviour of pyrazine carbohydrazide: Gravimetric, electrochemical, surface and theoretical study. *J. Mol. Liq.* **2020**, *299*, 112160. [CrossRef]
16. Verma, C.; Obot, I.; Bahadur, I.; Sherif, E.-S.M.; Ebenso, E.E. Choline based ionic liquids as sustainable corrosion inhibitors on mild steel surface in acidic medium: Gravimetric, electrochemical, surface morphology, DFT and Monte Carlo simulation studies. *Appl. Surf. Sci.* **2018**, *457*, 134–149. [CrossRef]
17. Alibakhshi, E.; Ramezanzadeh, M.; Bahlakeh, G.; Ramezanzadeh, B.; Mahdavian, M.; Motamedi, M. Glycyrrhiza glabra leaves extract as a green corrosion inhibitor for mild steel in 1 M hydrochloric acid solution: Experimental, molecular dynamics, Monte Carlo and quantum mechanics study. *J. Mol. Liq.* **2018**, *255*, 185–198. [CrossRef]
18. Stern, M.; Geaby, A.L. Electrochemical Polarization. *J. Electrochem. Soc.* **1957**, *104*, 56–63. [CrossRef]
19. Benoist, D.; Tourbier, Y.; Germain-Tourbier, S. *Designs D'expériences: Construction et Analyse*; Technique & Documentation, Lavoisier: Paris, France, 1994; ISBN 978-2-8520-6988-6.

20. Goupy, J. *Pratiquer les Designs D'experiences*; Dunod: Paris, France, 2017; ISBN 2-10-004217-3.
21. M'hanni, N.; Galai, M.; Anik, T.; Touhami, M.E.; Rifi, E.H.; Asfari, Z.; Touir, R. Influence of additives selected calix[4]arenes on electroless copper plating using hypophosphite as reducing agent. *Surf. Coat. Technol.* **2017**, *310*, 8–16. [CrossRef]
22. Galai, M.; Ouassir, J.; Ebn Touhami, M.; Nassali, H.; Benqlilou, H.; Belhaj, T.; Berrami, K.; Mansouri, I.; Oauki, B. α-Brass and (α+β) brass degradation processes in Azrou soil medium used in plumbing devices. *J. Bio- Tribo-Corros.* **2017**, *3*, 30. [CrossRef]
23. Zheng, X.; Zhang, S.; Li, W.; Yin, L.; He, J.; Wu, J. Investigation of 1-butyl-3-methyl-1H-benzimidazolium iodide as inhibitor for mild steel in sulfuric acid solution. *Corros. Sci.* **2014**, *80*, 383–392. [CrossRef]
24. Hegazy, M.A.; Abdallah, M.; Awad, M.K.; Rezk, M. Three novel di-quaternary ammonium salts as corrosion inhibitors for API X65 steel pipeline in acidic solution. Part I: Experimental results. *Corros. Sci.* **2014**, *81*, 54–64. [CrossRef]
25. Mathieu, D.; Nony, J.; Phan-Tan-Luu, R. *NEMROD-W Software*; LPRAI: Marseille, France, 2000.
26. Heakal, F.E.T.; Fouda, A.S.; Radwan, M.S. Some new thiadiazole derivatives as corrosion inhibitors for 1018 carbon steel dissolution in sodium chloride solution. *Int. J. Electrochem. Sci.* **2011**, *6*, 3140–3163. [CrossRef]
27. *ASTM G 81-97a*; Standard Test Method for Jaw Crusher Gouging Abrasion Test. ASTM International: West Conshohocken, PA, USA, 2007.
28. Murakawa, T.; Hackerman, N. The double layer capacity at the interface between iron and acid solutions with and without organic materials. *Corros. Sci.* **1964**, *4*, 387–396. [CrossRef]
29. Allabergenov, K.D.; Kurbanov, F.K. Acetylene Compounds—Inhibitors of Steel Corrosion in Sulfuric Acid. *Zashch. Met.* **1979**, *15*, 472–473.
30. Rengamani, S.; Muralidharan, S.; Anbu Kulandainathan, M.; Venkatakrishna Iyer, S. Inhibiting and accelerating effects of aminophenols on the corrosion and permeation of hydrogen through mild steel in acidic solutions. *J. Appl. Electrochem.* **1994**, *24*, 355–360. [CrossRef]
31. Bockris, J.M.; Yang, B. The mechanism of corrosion inhibition of iron in acid solution by acetylenic alcohols. *J. Electrochem. Soc.* **1991**, *138*, 2237. [CrossRef]
32. Hackerman, N.; Snavely, E.S., Jr.; Fiel, L.D. The anodic polarization behaviour of metals in hydrogen fluoride. *Corrosion Science* **1967**, *7*, 39–50. [CrossRef]
33. Oskes, G.; Vest, J.M. Influence of Thiourea on the Dissolution of Mild Steel in Strong Hydrochloric Acid. *Br. Corros. J.* **1969**, *4*, 66–73.
34. MAmin, M.A.; Abd El-Rehim, S.S.; El-Sherbini, E.E.F.; Bayoumi, R.S. The inhibition of low carbon steel corrosion in hydrochloric acid solutions by succinic acid: Part I. Weight loss, polarization, EIS, PZC, EDX and SEM studies. *Electrochim. Acta* **2007**, *52*, 3588–3600.
35. Lenderink, H.J.W.; Linden, M.V.D.; De Wit, J.H.W. Corrosion of aluminium in acidic and neutral solutions. *Electrochim. Acta* **1993**, *38*, 1989–1992. [CrossRef]
36. Amin, M.A.; Khaled, K.F.; Mohsen, Q.; Arida, H.A. A study of the inhibition of iron corrosion in HCl solutions by some amino acids. *Corros. Sci.* **2010**, *52*, 1684–1695. [CrossRef]
37. Alaoui, K.; El Kacimi, Y.; Galai, M.; Serrar, H.; Touir, R.; Kaya, S.; Kaya, C.; Touhami, M.E. New triazepine carboxylate derivatives: Correlation between corrosion inhibition property and chemical structure. *Int. J. Ind. Chem.* **2020**, *11*, 23–42. [CrossRef]
38. Prabakaran, M.; Kim, S.H.; Mugila, N.; Hemapriya, V.; Parameswari, K.; Chitra, S.; Chung, I.M. Aster koraiensis as nontoxic corrosion inhibitor for mild steel in sulfuric acid. *J. Ind. Eng. Chem.* **2017**, *52*, 235–242. [CrossRef]
39. Sherif, E.S.M.; Erasmus, R.M.; Comins, J.D. Inhibition of copper corrosion in acidic chloride pickling solutions by 5-(3-aminophenyl)-tetrazole as a corrosion inhibitor. *Corros. Sci.* **2008**, *50*, 3439–3445. [CrossRef]
40. El Mehdi, B.; Mernari, B.; Traisnel, M.; Bentiss, F.; Lagrenee, M. Synthesis and comparative study of the inhibitive effect of some new triazole derivatives towards corrosion of mild steel in hydrochloric acid solution. *Mater. Chem. Phys.* **2003**, *77*, 489–496. [CrossRef]
41. El-Hajjaji, F.; Messali, M.; Aljuhani, A.; Aouad, M.; Hammouti, B.; Belghiti, M.; Chauhan, D.; Quraishi, M. Pyridazinium-based ionic liquids as novel and green corrosion inhibitors of carbon steel in acid medium: Electrochemical and molecular dynamics simulation studies. *J. Mol. Liq.* **2018**, *249*, 997–1008. [CrossRef]
42. Singh, A.K.; Quraishi, M.A. Effect of 2, 2′ benzothiazolyl disulfide on the corrosion of mild steel in acid media. *Corros. Sci.* **2009**, *51*, 2752–2760. [CrossRef]
43. Prabhu, R.; Venkatesha, T.; Shanbhag, A.; Kulkarni, G.; Kalkhambkar, R. Inhibition effects of some Schiff's bases on the corrosion of mild steel in hydrochloric acid solution. *Corros. Sci.* **2008**, *50*, 3356–3362. [CrossRef]
44. El Caid, Z.A.; Left, D.B.; Thoume, A.; Kellal, R.; Zertoubi, M. A Comprehensive Computational Study of N-Phenylacetamide Derivatives as Corrosion Inhibitors for Copper: Insights from DFT and Molecular Dynamics. *J. Bio- Tribo-Corros.* **2023**, *9*, 83. [CrossRef]
45. Singh, A.K.; Quraishi, M.A. The effect of some bis-thiadiazole derivatives on the corrosion of mild steel in hydrochloric acid. *Corros. Sci.* **2010**, *52*, 1373–1385. [CrossRef]

46. Ashassi-Sorkhabi, H.; Seifzadeh, D.; Hosseini, M.G. EN, EIS and polarization studies to evaluate the inhibition effect of 3H-phenothiazin-3-one, 7-dimethylamin on mild steel corrosion in 1 M HCl solution. *Corros. Sci.* **2008**, *50*, 3363–3370. [CrossRef]
47. Tao, Z.; Zhang, S.; Li, W.; Hou, B. Corrosion inhibition of mild steel in acidic solution by some oxo-triazole derivatives. *Corros. Sci.* **2009**, *51*, 2588–2595. [CrossRef]
48. Verma, C.; Olasunkanmi, L.O.; Obot, I.B.; Ebenso, E.E.; Quraishi, M.A. 5-Arylpyrimido-[4,5-b]quinoline-diones as new and sustainable corrosion inhibitors for mild steel in 1 M HCl: A combined experimental and theoretical approach. *RSC Adv.* **2016**, *6*, 15639–15654. [CrossRef]

Disclaimer/Publisher's Note: The statements, opinions and data contained in all publications are solely those of the individual author(s) and contributor(s) and not of MDPI and/or the editor(s). MDPI and/or the editor(s) disclaim responsibility for any injury to people or property resulting from any ideas, methods, instructions or products referred to in the content.